Exhaustive list of topological hourglass band crossings in 230 space groups

Lin Wu, Feng Tang,* and Xiangang Wan
National Laboratory of Solid State Microstructures and School of Physics, Nanjing University, Nanjing 210093, China
and Collaborative Innovation Center of Advanced Microstructures, Nanjing University, Nanjing 210093, China

(Received 27 January 2020; revised 19 May 2020; accepted 8 June 2020; published 2 July 2020)

Topological semimetals with band crossings (BCs) near the Fermi level have attracted intense research activity in the past several years. Among various BCs, those enforced by an hourglasslike connectivity pattern, which are located just at the vertex in the neck of an hourglass and thus called hourglass BCs (HBCs), show interesting topological properties and are intimately related with the space group symmetry. Through checking compatibility relations in the Brillouin zone, we list all possible HBCs for all 230 space groups by identifying positions of HBCs as well as the compatibility relations related with the HBCs. The HBCs can be compatible with conventional topological BCs such as Dirac and Weyl fermions and, based on our exhaustive list, the dimensionality and degeneracy of the HBCs can be quickly identified. It is also found that the HBCs can be classified into two categories: one contains essential HBCs which are guaranteed to exist, while the HBCs in the other category may be tuned to disappear. Our results can help in efficiently predicting hourglass semimetals combined with first-principles calculations as well as studying transitions among various topological crystalline phases.

DOI: 10.1103/PhysRevB.102.035106

I. INTRODUCTION

In the past decade, there has been persistent and extensive research interest in both theoretical and experimental studies on topological materials because of their values in both fundamental and applied research [1–5]. On one hand, theorists attempt to classify symmetry-protected topological phases in a unified frame as much as possible [6–9]. On the other hand, many kinds of topological materials, insulators, or metals were proposed with specific topological properties [1–5] and material realizations for them were oftentimes predicted through first-principles calculations and then verified by experiments [1–5].

Among various topological materials, topological semimetals [5] with nontrivial band crossings (BCs) have attracted much attention since Weyl semimetals were proposed and predicted to be able to host exotic surface states and novel quantum responses [5,10–13]. Other than Weyl semimetals where the twofold Weyl BC can occur even without symmetry protection, various topological semimetals were proposed where the relevant BCs are protected by crystallographic symmetry operations. With BCs distinguishable in dimensionality, degeneracy, or connection patterns, Dirac semimetals [14–17], topological semimetals with multifold-degenerate BCs [18–22], nodal line semimetals [23–27], nodal-chain semimetals [28], Hopf-link semimetals [29–32], and so on were born.

One type of topological semimetals, named hourglass semimetals [33–42], has attracted much attention recently. In an hourglass semimetal, the hourglass BC forms due to a hourglasslike band connectivity in the bulk Brillouin zone (BZ) as shown in Figs. 1(a)–1(e). To our best knowledge, material realizations of such hourglass fermions to date were mostly studied in orthorhombic crystal systems, for example, $Li_3(FeO_3)_2$ [space group (SG) 34, *Pnn2*] [43], Ag_2BiO_3 (SG 52, *Pnna*) [44,45], ReO_2 (SG 60, *Pbcn*) [35], $SrIrO_3$ [36], Ta_3SiTe_6 and Nb_3SiTe_6 (SG 62, *Pbmn*) [46], AgF_2 (SG 61, *Pbca*) [47,48], and $BaLaCuBO_5$(SG 100, *P4bm*) [49].

It is worth pointing out that hourglass BCs can be topological BCs, which have been extensively studied. For example, the hourglass BCs are allowed to own Weyl-like band topology, namely, a finite monopole charge, but such an hourglass Weyl point has to be located within special positions of the BZ. Other than the hourglass Weyl point, the hourglass BC can also be a Dirac point. However, the hourglass BCs needn't be pinned down to high-symmetry points (HSPs) [14,18] and can be movable in the high-symmetry line (HSL). In addition, the hourglass BCs could be robust against external perturbation as long as the perturbation preserves the symmetry, since the band inversion in the hourglass BC is usually enforced to occur [33–37]. The hourglass BC can also lie in a nodal line. Furthermore, when each point of a nodal line is an hourglass BC, the nodal line is thus called hourglass nodal line. To date, the studies on hourglass semimetals are all based on a specific kind of symmetry setting [33–37]. However, an exhaustive study on hourglass BCs in all 230 SGs could stimulate predicting and studying coexisting different types of topological hourglass BCs and provide a complete searching or design principle for realistic hourglass materials as well.

In this paper, we use the compatibility relations in the 230 SGs as listed on the Bilbao server [50] to obtain all possible and concrete positions in the BZ which allow hourglass BCs in the electronic band structures. These results consider

*Corresponding author: fengtang@nju.edu.cn

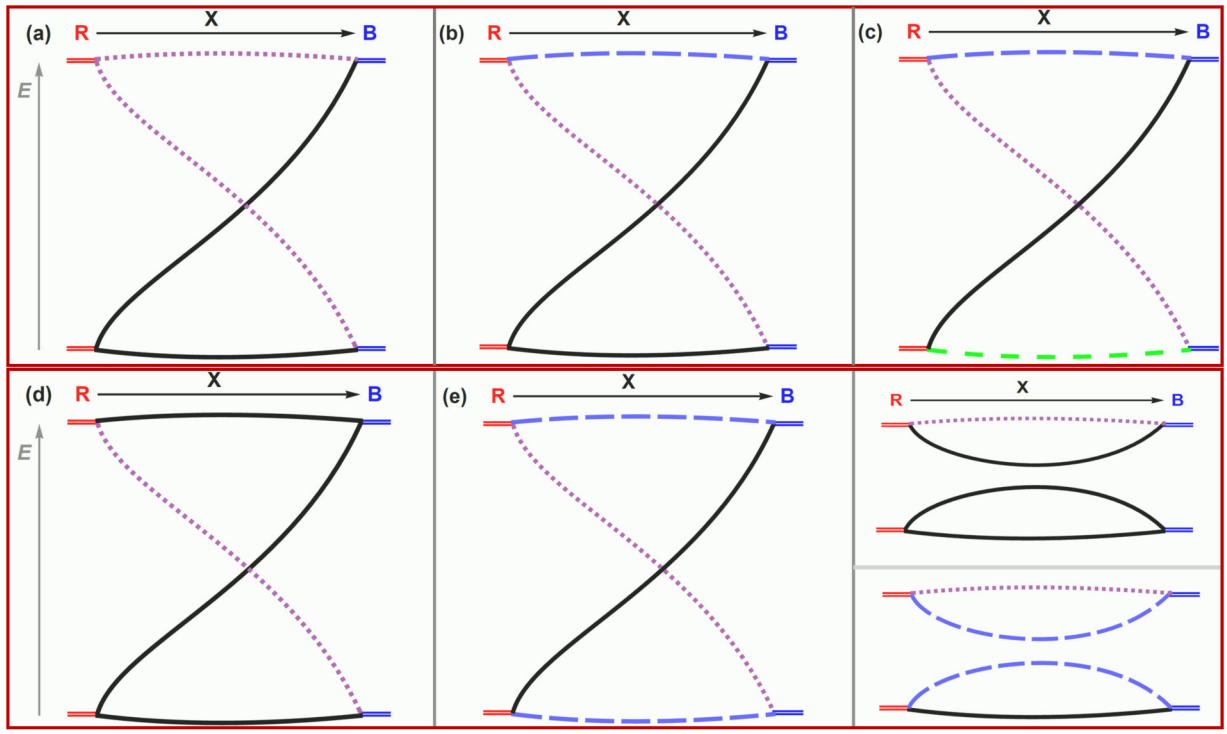

FIG. 1. Classification of the hourglass band structures: (a)–(e) correspond to hourglass BCs of types a–e, respectively. R, B denote two (sets of) **k** vectors in the BZ which must be HSP or HSL while X, which can be HSL or HSPL, connects R and B. Energy bands from R to X split according to the compatibility relations. For stable band crossings as shown in the neck of hourglass, X must allow two different irreps, as indicated by black solid and purple dotted lines. For types a–c, the numbers of additional involved irreps other than the two irreps in then neck for the bottom and top bands are 0, 1, 2, respectively, as indicated by different colors and styles of lines. It is easy to find that these hourglass band structures are stable against switching band orderings of R or B, owing to different irreps in the bottom and top bands. However, the remaining two hourglass structures in d and e can be tuned to gapped as shown in the last panel since the bottom and top bands share the same irrep. Note that for types a–c, once for R and B, all possible splitting patterns in X are and can only be those as displayed, the hourglass band connectivity must exist since the partner switch of any Bloch states have to happen to satisfy the compatibility relations, thus they are essential.

four settings[with/without time-reversal symmetry (TRS) and with significant/negligible spin-orbit coupling (SOC)]. We find that the hourglass dispersion can occur in all crystal systems other than the triclinic crystal system [since no HSL or high-symmetry plane (HSPL) exists for triclinic crystal system]. An interesting finding is that even in symmorphic SG, an hourglass band structure also has a chance to appear as listed in Table II while they are all nonessential.

TABLE I. All possible combinations of R, X, and B which can host hourglass band crossings in X connecting R and B. The nodal line among the table may not be the hourglass structure because it is possible that not all the points constituting the nodal line are originated from hourglass crossings.

R	X	B	Property of HBC
HSP	HSL	HSP	Hourglass nodal point or lying in a nodal line
HSP	HSPL	HSP	Hourglass nodal line
HSP	HSPL	HSL	Hourglass nodal line
HSL	HSPL	HSL	Hourglass nodal line

TABLE II. All positions of nonessential hourglass BCs in symmorphic SGs. The first column contains labels for X and, in the second column, it contains several SG numbers which could allow nonessential hourglass BCs in the corresponding HSLs. The types of these hourglass BCs are also given.

X	SG
	Time-reversal symmetric, neglecting SOC
LD	e:215,217,221,229
DT	e:217,229
A	a:221,225,229
B	a:221
Z	c:221
	Time-reversal symmetry broken, considering SOC
LD	e:195,197,200,204
	Time-reversal symmetry broken, neglecting SOC
LD	e:215,217,221,229
DT	e:229
A	a:221,225,229
B	a:221
Z	c:221

TABLE III. All positions of HSLs for essential hourglass nodal points. The first column contains labels for the HSLs (X) and the second column contains several SG numbers which could allow essential hourglass nodal points in the corresponding HSLs. The letters a and c denote the essential hourglass nodal points with type-a and type-c BCs, respectively. Note that here type x means that there is only one hourglass structure of type x, as distinguished from type a+ type a hourglass BC in Fig. 2 where two different hourglass structures of type a exist. Chiral SGs are printed in bold and the SGs are in red, to which the materials discussed in the main text belong.

X	SG
	Time-reversal symmetric, considering SOC
LD	a: **4**,**17**,**19**,**20**; c: **77**,**80**,**93**, **94**,**98**
U	a:**4**, **90**, **94**, 113, 130, 138, **169**, **170**, **173**, **178**, **179**,182
V	a: **4**, 106, 133, 219;c:**77**,**93**
W	a:**4**, **76**, **78**, **91**, **95**, 120
G	a:**17**
H	a:**17**,**20**,60
Q	a:**17**
A	a:**18**,54,56
B	a:**18**,56
DT	a:**18**, **19**, **90**, **92**, **94**, **96**, 113, 114
SM	a:**18**, **19**
D	a:**20**,36, 52
P	a:45
E	a:54
	Time-reversal symmetry broken, considering SOC
LD	c:93, 94, 98
V	c:93, 94

In Tables III and IV of the main text, we list all the positions of essential hourglass nodal points and nodal lines in all four settings, respectively. These essential results all belong to nonsymmorphic SGs. It is worth pointing out that, with regard to essential hourglass BCs, as long as a material crystallizes in SG as listed in Tables III and IV, the hourglass band structure would always exist in the positions in the BZ shown in Tables III and IV, regardless of the chemical composition. Hence, our results can be used to predict materials with topological hourglass excitations around the Fermi level efficiently.

This paper is organized as follows. In Sec. II, we first enumerate all possibilities or types of hourglass BCs based on which we propose criteria or necessary conditions on compatibility relations or a splitting pattern of existence for all types of hourglass BCs. Based on the necessary conditions, we obtain a large number of possible hourglass BCs and list them in the Supplemental Material (SM) [51]. Then in Sec. III, we further impose an additional condition to obtain essential hourglass BCs. We list all concrete positions in the BZ of essential hourglass nodal points and nodal lines in Tables III and IV, respectively. Based on these tables, we demonstrate three hourglass materials whose electronic band structures are calculated by first-principles calculations in Sec. IV and two others shown in the SM [51] (see also Refs. [52–55] therein). Conclusions and perspectives are given in Sec. V.

TABLE IV. All positions of HSPLs for essential hourglass nodal lines. The first column contain labels for the HSPLs (X) and the second column contains several SG numbers which could allow essential hourglass nodal lines in the corresponding HSPLs. The letter a means that the essential hourglass nodal line is within type-a hourglass BC. SG 62 (printed in red) is used to show an hourglass nodal line material in the main text.

X	SG
	Time-reversal symmetric, considering SOC
F	a: 7, 102, 104, 118
G	a:7
B	a: 9, 45, 46, 100, 102, 104, 106, 108, 110, 117, 118, 120
K	a:26, 30, 31, 32, 33, 34, 36
L	a:26, 29, 30, 33, 34, 60, 61, 62
M	a:28, 29, 31, 32, 33, 34, 40, 41
N	a:28, 29, 30, 31, 34, 57, 61
P	a:39, 41
Q	a:39, 41
E	a:43
J	a:43
A	a:45, 109, 110, 122
W	a:60,61
D	a:158,186,188
C	a:159, 161, 185, 190, 220
	Time-reversal symmetric, neglecting SOC
L	a:29, 33, 52, 57
M	a:29, 33, 54, 56, 60, 61
N	a:29, 54, 60
V	a:52, 61, 62
W	a:54, 56
K	a:56, 57, 60, 61
B	a:130, 138
E	a:130, 135, 138
A	a:205
	Time-reversal symmetry broken, considering SOC
K	a:48, 62
L	a:48, 50, 52, 60, 61, 62
M	a:48, 52, 70
N	a:48, 50, 57, 60, 61
V	a:48, 50, 56, 59
W	a:48, 50, 52, 54, 56, 59, 60, 61
Q	a:68
E	a:70, 126, 130, 132, 133, 137
J	a:70
F	a:125, 126, 133, 134
B	a:126, 134, 201, 222
A	a:201
	Time-reversal symmetry broken, neglecting SOC
L	a:52, 54, 56, 57
N	a:52, 54, 56
V	a:52, 61, 62
M	a:54, 56, 60, 61
K	a:56, 57, 60, 61
W	a:60, 62
B	a:130, 138
F	a:130, 138
E	a:135
A	a:205

II. CRITERIA OF HOURGLASS BAND CROSSING: NECESSARY CONDITIONS

In the BZ, any wave vector can be classified by its symmetry into an HSP, a point lying in an HSL or HSPL, and a generic point without any symmetry. Obviously, hourglass BCs can only appear in HSL or HSPL for which two different irreducible representations (irreps) are allowed. Such a HSL or HSPL hosting an hourglass BC is denoted by X from here on. In the following, we would outline all the necessary conditions for the formation of an hourglass BC.

First, we describe the property of wave vectors related with any hourglass BC. Any hourglass structure consists of four sets of energy bands in X as shown in Figs. 1(a)–1(e): the four sets of bands connect two energy levels at R and B in a zigzag manner. Here R or B are connected by X, providing two energy levels splitting in X. Thus for each hourglass BC, R-X-B should be specified. All possible combinations of R-X-B are given in Table I. Many examples of R-X-B can be found in Secs. II– V of the SM [51]; for example, with respect to T-K-GM in SG 32, where $T = (0, \frac{1}{2}, \frac{1}{2})$, $K = (0, v, w)$ and GM=(0,0,0), it is easy to find that K connects T and GM. Note that we exactly follow the name convention of wave vectors on the Bilbao server [50] where all the coordinates in the conventional basis can also be found. Interestingly, when X is an HSPL, there would be an infinite number of paths in X connecting R and B, each of which contributes an hourglass BC, thus resulting in an hourglass nodal line. However, when X is a HSL, we should pay some attention.

(1) If no HSPL contains X, the hourglass BC in X must be an (symmetry-allowed) hourglass nodal point, that is to say, the band touching in hourglass BC in X cannot survive in any direction away from the BC.

(2) On the contrary, if we can find one or several HSPLs containing X, then we should check that if there exist(s) one or several HSPLs containing X, satisfying that the two different irreps of the hourglass BC can still maintain being two different irreps in these HSPLs. If that is true, the hourglass BC in X would lie in a nodal line in the corresponding HSPLs. Otherwise, the hourglass BC in X is an hourglass nodal point.

Thus, for X being an HSL, it is still possible to obtain a nodal line threading the hourglass BC in X. We find that such a case usually (but not always) indicates existence of another HSPL, denoted by X′, hosting a hourglass nodal line and $X \in X'$. For example, from Sec. II of the SM [51], SG 62 could host an hourglass BC in D (an HSL) connecting S and X. However, we further find that such a BC actually lies in a nodal line within an HSPL, L (and $D \in L$). In fact, L itself can host an hourglass nodal line. However, such X′ not always exists, with the counterexample being SG 205 [51]: the only possible hourglass BC in an HSL, $ZA \in B$ (an HSPL), is found to lie in a nodal line within B, but B cannot host hourglass nodal line.

An important characteristic of the hourglass structure is that the band inversion of a BC arises from a state-switching process from R to B through X. This can be illustrated in detail as follows. Assume that there has existed an hourglass BC in R-X-B, so the properties it has thus provide necessary conditions to realize hourglass BCs. Since the little group of X must be a subgroup of R or B, the energy level at R or B may split in X, according to the compatibility relations of irreps between R or B and X [50]. It is easy to find that R and B should allow a degenerate energy level which is able to split to two and only two sets of bands, corresponding to two irreps in X (note that these two irreps may be the same one). We emphasize that we needn't care about which irrep at R and B of the aforementioned energy level splits to irreps in X, and what matters essentially is how bands that originated from R or B split in X, called a splitting pattern, which can be obtained from the compatibility relation given on the Bilbao server [50]. As shown Figs. 1(a)–1(e), two energy levels at R and B split in X; we can thus use the notation as

$$\mathrm{X}_i \oplus \mathrm{X}_j, \mathrm{X}_{i'} \oplus \mathrm{X}_{j'}; \mathrm{X}_{i''} \oplus \mathrm{X}_{j''}, \mathrm{X}_{i'''} \oplus \mathrm{X}_{j'''} \tag{1}$$

to specify the splitting pattern in any hourglass structure where $i, j, i', j', \ldots$ denote the irreps in X. The two splitting patterns before (after) the semicolon correspond to higher and lower energy levels at R (B), respectively. To be specific, $\mathrm{X}_i \oplus \mathrm{X}_j$ means that the higher energy levels at R split to irreps X_i and X_j; $\mathrm{X}_{i'} \oplus \mathrm{X}_{j'}$ means that the lower energy levels at R split to irreps $\mathrm{X}_{i'}$ and $\mathrm{X}_{j'}$; $\mathrm{X}_{i''} \oplus \mathrm{X}_{j''}$ means that the higher energy levels at B split to irreps $\mathrm{X}_{i''}$, and $\mathrm{X}_{j''}$ and $\mathrm{X}_{i'''} \oplus \mathrm{X}_{j'''}$ means that the lower energy levels at B split to irreps $\mathrm{X}_{i'''}$ and $\mathrm{X}_{j'''}$.

Note that the irreps in X participating in an hourglass structure cannot be chosen arbitrarily and should satisfy certain constraints as shown below. First of all, $\mathrm{X}_i \oplus \mathrm{X}_j$ cannot be equal to $\mathrm{X}_{i''} \oplus \mathrm{X}_{j''}$, otherwise they could be connected with each other, violating the hourglass band connectivity. So $\mathrm{X}_i \oplus \mathrm{X}_j \neq \mathrm{X}_{i''} \oplus \mathrm{X}_{j''}$, thus the states from lower energy should have to be incorporated, as shown later, to result in a switch of different irreps in X, which enforces an hourglass BC.

Next, we list all possible cases of the splitting patterns in X for an hourglass BC in R-X-B shown in Figs. 1(a)–1(e). With no loss of generality, we label the different irreps for the BC in the neck of the hourglass as X_1 and X_2, which are represented by a black solid line and purple dashed line, respectively, as in Figs. 1(a)–1(e). Then, considering the irreps for the bottom and top part of the hourglass, we obtain all five possibilities as follows:

Type a: The irreps of the bottom and top parts are different but they share the same irreps as those of the neck parts. We can denote the top irrep as X_2, as in Fig. 1(a). Note that the other choice of the top irrep being X_1 would give the same type of hourglass (just reversing the order of R and B). Hence, the splitting patterns can be denoted as $2\mathrm{X}_2$, $2\mathrm{X}_1$; $\mathrm{X}_1 \oplus \mathrm{X}_2$, $\mathrm{X}_1 \oplus \mathrm{X}_2$. It is easy to find that X_1 and X_2 have been interchanged between R and B by this formal notation: The higher energy levels of R and B cannot be directly connected since they contain different irreps in X (i.e., $2\mathrm{X}_2 \neq \mathrm{X}_1 \oplus \mathrm{X}_2$) as well as the lower energy levels. The states in the higher and lower energy levels at R interchange X_1 and X_2 in X and finally change to those at B.

Type b: The same as type a, the irreps of the bottom and top parts are different but they only share one common irrep with those of the neck parts. Denote the common irrep as X_1 for the bottom band and the other irrep for the top band is X_3. The splitting patterns are thus $\mathrm{X}_2 \oplus \mathrm{X}_3$, $2\mathrm{X}_1$; $\mathrm{X}_1 \oplus \mathrm{X}_3$, $\mathrm{X}_1 \oplus \mathrm{X}_2$. From this formal notation, X_1 and X_2 is interchanged from

R and B through X, which are just the irreps participating in the hourglass BC.

Type c: The irreps of the bottom and top parts are different and they share no common irrep with those of the neck parts. Denote the irrep as X_4 for the bottom band and the other irrep for the top band is X_3. The splitting patterns are thus $X_2 \oplus X_3$, $X_1 \oplus X_4$; $X_1 \oplus X_3$, $X_2 \oplus X_4$.

Type d: Different from the above three types, for this type, the bottom and top bands share the same irrep in X which is X_1 or X_2. We can denote the irrep of the bottom and top bands as X_1. Thus the splitting patterns are $X_1 \oplus X_2$, $2X_1$; $2X_1$, $X_1 \oplus X_2$.

Type e: The bottom and top bands share the same irrep in X which is not X_1 or X_2. We can denote the irrep of the bottom and top bands as X_3. Thus the splitting patterns are $X_2 \oplus X_3$, $X_1 \oplus X_3$, and $X_1 \oplus X_3$, $X_2 \oplus X_3$.

The hourglass BCs of the above five types are schematically shown in Figs. 1(a)–1(e), respectively. The degeneracy of the hourglass BC is simply the sum of the dimension of the two interchanged irreps X_1 and X_2. Different from the hourglass BCs of types a–c, the hourglass BCs of types d and e can be gapped by interchanging the band ordering in R or B. For example, with respect to hourglass BC of type d, when interchanging the band ordering at R, the splitting patterns are thus: $2X_1$, $X_1 \oplus X_2$; $2X_1$, $X_1 \oplus X_2$. Hence the higher and lower energy levels can both be directly connected from R and B through X without any state switch and a continuous energy gap could exist to separate the four sets of bands. The effect of interchanging energy levels R or B or both R and B for all five types giving equivalent hourglass band structures are displayed in Fig. 1 of the SM [51].

It is also worth pointing out that even for types a–c shown in Fig. 1, the hourglass BCs can be tuned to disappear when another kind of splitting pattern(s) with common irrep(s) shared in the hourglass structure are incorporated. Here we show a specific example of this situation, shown in Fig. 2, where two hourglasses in type a are formed in the left panel of Fig. 2(b) but can be tuned to be gapped as shown in the right panel of Fig. 2(b). In this example, as a matter of fact, it is found that although the hourglasses satisfy the compatibility relations or splitting patterns for hourglass BC of type a with respect to the band orderings at V_1, shown in Fig. 2(a), V can allow another splitting pattern which could accommodate and directly connect the bands originating from A without any BCs. This can be done by changing the band ordering shown in V_2 of Fig. 2(a) to realize the direct connections. It's understood that what we proposed are necessary conditions, given the hourglass BC has been formed, while they can also be gapped or coexist with other kinds of band connectivity.

Based on the necessary conditions for types a–e, namely, the splitting patterns required by a specific type are allowed by the compatibility relations, we exhaustively investigate the compatibility relations listed on the Bilbao server [50] and obtain comprehensive results all listed in Secs. III, IV, V, and VI of the SM [51], including the SG, R-X-B, related splitting pattern as Eq. (1), dimensionality (nodal line or point), and the type. It is understandable that the majority of the results are of type-a hourglass BCs since only two different irreps are required for X in this type. Even though those results may not essentially (i.e., accidently) guarantee an hourglass structure, they can indeed provide the possibility of an hourglass BC and can also aid in designing structures to tune hourglass structure(s) to be gapped or even transform to other types of BCs. It is interesting to find that in several symmorphic SGs, hourglass BCs could occur as listed in Table II and these BCs are all nonessential, namely, they can be tuned to be gapped by strong external strains which change the band orderings at R or B.

III. SUFFICIENT CONDITION FOR ESSENTIAL HOURGLASS BAND CROSSING AND RESULTS

The tables of Secs. II, III, IV, and V of the SM [51] contain many essential hourglass BCs of a specific type (as printed in red there), which can be applied to predict materials with topological hourglass excitations near the Fermi level. In this section, we describe our additional condition other than the above necessary conditions, which could guarantee that the hourglass BC is essential, that is, they must exist, cannot be gapped, and are the only kind of possible band connectivity. To obtain an essential hourglass BC in R-X-B, obviously, it should allow splitting patterns in type a, b, or c since hourglass BCs of types d and e can be tuned to be gapped as shown in the last panel of Fig. 1. Furthermore, the following condition should be satisfied:

No other splitting patterns exist other than those required for type a, b, or c.

It is worth pointing out that we have checked our results and actually find that it is possible to realize several essential hourglass BCs of different types or with different combinations of splitting patterns for the same type. However, only the HSL G in SGs 29 and 33 and the HSL DT in SGs 173 and 182 (for all that, TRS and SOC are both considered) can host such special essential hourglass BCs. Hence, when we say essential type-x hourglass BC, it means that there is only one such hourglass BC of type x (= a, b, c) exclusively.

By the above additional requirement, we filter out nonessential hourglass BCs and those essential hourglass nodal points and nodal lines, and they are collected in Tables III and IV, respectively, where only X is specified. The concrete coordinates of X as well as the splitting patterns (so the degeneracy of hourglass BC can be obtained) can be found in the SM [51].

Here we take SG 182 as an example to illustrate the essential hourglass BC. By checking all the compatibility relations for SG 182 listed on the Bilbao sever [50], we can see that there is an essential hourglass nodal point of type a on the HSL U which connects two HSPs L and M when TRS and SOC are both considered. Here we label these irreps with the same convention in Ref. [50]. The irreps of U include two one-dimensional irreps U3 and U4. Meanwhile, there are two two-dimensional irreps L2, 4 (here 2,4 means that the irreps 2 and 4 for L are paired by TRS to give the coirrep) and L3, 5 at point L and there is only one two-dimensional irrep M5 at point M. The irreps at L are found to be related with those in U, according to the compatibility relations as follows [50]:

$$\begin{aligned} \mathrm{L2,4} &\rightarrow \mathrm{2U3}, \\ \mathrm{L3,5} &\rightarrow \mathrm{2U4}, \end{aligned} \tag{2}$$

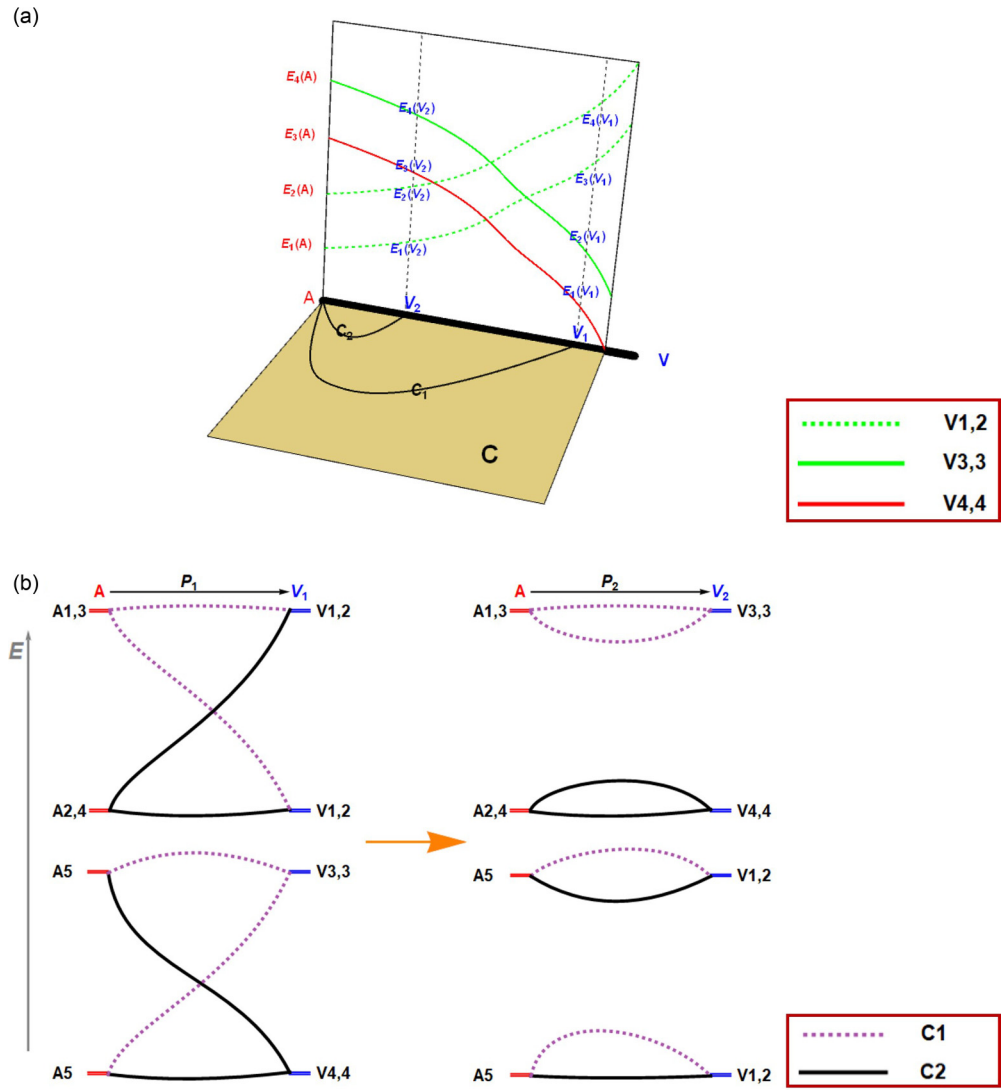

FIG. 2. When two different hourglass structures both of type a (see Fig. 1), called type a+type a hourglass BC, have existed, they can still be turned to be gapped through tuning the band orderings. Here we show a concrete example in SG 113 when considering TRS and neglecting SOC, any point in the HSL V can own three two-dimensional irreps (labeled V1,2; V3,3; and V4,4; indicated by dashed green, solid green, and solid red lines, respectively). The HSP A can also host three 2-dimensional irreps (labelled by A1,3, A2,4 and A5). The compatibility relations between A and V are A1,3→ V3,3, A2,4→ V4,4 and A5→ V1,2. The HSPL C could only own two one-dimensional irreps: C1 and C2. Consider four bands (all are twofold degenerate) crossing as in (a). Thus, when considering the path C_1 in C connecting A and V_1 in V, there would be two hourglass structures both of type a shown in the left panel of (b) due to the compatibility relations for the energy levels in order at A and V_1: A5→ C1+C2, A5→ C1+C2, A1,3→2C1, A2,4→ 2C2 and V4,4→2C2, V3,3→2C1, V1,2→ C1+C2, V1,2→ C1+C2. However, for another path C_2 connecting A and V_2, the hourglasses disappear since the energy levels at V_2 allow the direct connection of the four energy levels, according to the compatibility relations.

while for M, we have [50]

$$\mathrm{M5} \rightarrow \mathrm{U3} \oplus \mathrm{U4}. \tag{3}$$

The above compatibility relations obviously satisfy the requirement of hourglass BC type a. Furthermore, since all possible compatibility relations for L and U as well as M and U are shown above, there is only one (inequivalent) splitting pattern for L-U-M. Therefore, such an hourglass BC is essential and, furthermore, found to be an hourglass nodal point. We thus list U in Table III and assign 182 to it, meaning that U in SG 182 can host an essential hourglass nodal point. It can also be found that, other than 182, several other SGs such as SGs 4, 90, and 94 could also host an essential hourglass nodal point in U as read from Table III. In Sec. IV A, the electronic band structure of a realistic material in SG 182 is calculated by first principles, where the essential hourglass nodal points are explicitly demonstrated.

As shown in Tables III and IV, a notable feature of the essential results is that all nodal points, except in LD and V, and all nodal lines are of type a, i.e., only two different irreps are allowed in X. This is understandable since many HSLs or HSPLs can only host two different irreps at most. We also note that 12 SGs can host essential hourglass nodal points in more than one HSL or HSPL and 19 SGs host essential nodal lines in more than one HSPL; for example, SG 118 can host essential hourglass nodal lines in HSPLs B and F, so the

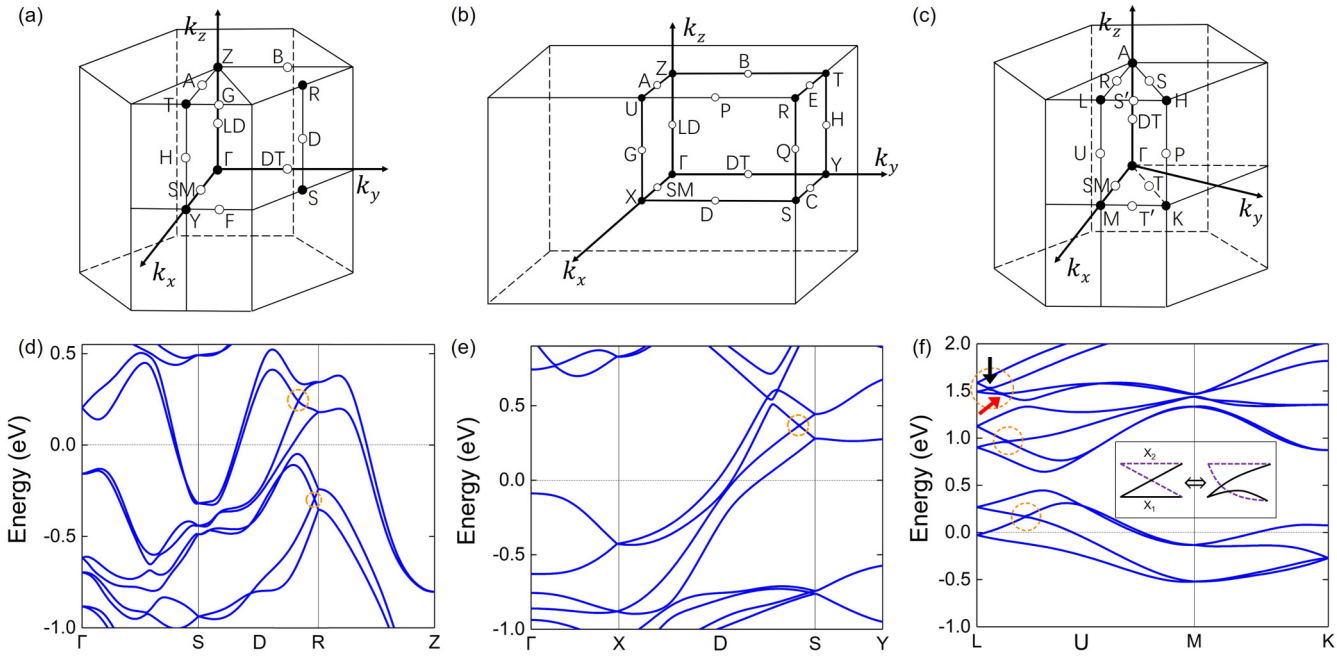

FIG. 3. (a) The BZ of base-centred orthorhombic lattice, where the labels of inequivalent HSPs and HSLs are given, following the notation adopted from the Bilbao server [50]. (b) The BZ of primitive orthorhombic lattice, where the labels of inequivalent HSPs and HSLs are given, following the notation adopted in the Bilbao server [50]. (c)The BZ of the trigonal lattice where we label all the inequivalent HSPs and HSLs following the Bilbao Server [50]. (d) Electronic band structure of $AsPb_2Pd_3$ (SG 36) by first principles calculations where S-D-R line could always host hourglass nodal points. S and R are two HSPs and D is HSL. Two such nodal points are circled by dashed curves almost near the Fermi level. (e)The first-principles calculated electronic band structure of Sr_2Bi_3(SG 52) with the hourglass nodal point indicated by orange dashed circle. (f) The principle-calculated electronic band structure of ReO_3 (SG 182) with three Weyl hourglass points indicated by dashed circles. Note that, for the highest circle, there exist two BCs, one (denoted by black arrow) is caused by hourglass structure and robust while the other one (denoted by the red arrow) is not robust and can be tuned to disappear as shown in the inset.

positions of those multiple nodal lines or loops in the BZ may affect the topological structure sensitively. In addition, there are 23 chiral SGs which are found to be able to host essential hourglass nodal points, for example, SG 90, could host a finite monopole charge [56].

Besides, as shown in Tables III and IV, essential hourglass nodal lines can occur in crystal systems other than triclinic crystal systems, while essential hourglass nodal points can emerge in crystal systems other than triclinic and trigonal systems. This indicates that hourglass materials could be ubiquitous in nature.

IV. MATERIAL REPRESENTATIVES

A. Materials with essential hourglass nodal points

As shown in Table III, for SG 36, D connecting HSPs S and R as shown in Fig. 3(a), could host an essential hourglass nodal point. The irreps of D are two one-dimensional irreps D3 and D4. Irreps at R or S are related with those in D as indicated by the compatibility relations. There are two two-dimensional irreps at point R which are reduced to 2D3 and 2D4. As R point, S point also allows two two-dimensional irreps, but they are both reduced to D3 ⊕ D4. Thus these splitting patterns satisfy the requirement of type-a hourglass BC. Furthermore, the hourglass BC in D is essential and found to be just an hourglass nodal point [51].

Similarly, for SG 52, D listed in Table III, connects HSPs S and X as shown in Fig. 3(b), and could also host essential hourglass nodal point as analyzed below. The irreps of D are two two-dimensional irreps D2, 4 and D3, 5. Two different splitting patterns for S to X are 2D2, 4 and 2D3, 5 while the only splitting pattern for point X to D is D2, 4 ⊕ D3, 5. Therefore, hourglass BC of type a could occur in D and the BC is found to be essential as in SG 36.

The above two SGs both own achiral operations, while SG 182 which is chiral, could host chiral hourglass nodal point in HSL U as shown in Table III: from L to U [see Fig. 3(c)], there are two possible splitting patterns 2U3 and 2U4, while from M to U [see Fig. 3(c)], the only splitting pattern is U3 ⊕ U4, as shown in Eqs. (2) and (3). Hence, an hourglass BC of type a could occur in U and is further found to be essential. As SG 182 is a chiral SG and U3 and U4 are both one-dimensional, then such an hourglass nodal point in U is a Weyl point.

First, we showcase $AsPb_2Pd_3$ [57] crystallizing in SG 36 with a base-centered orthorhombic lattice, whose first-principles calculated electronic band structures are shown in Fig. 3(d). As discussed above, the bands in S-D-R must host an hourglass nodal point. Clearly, the electronic band structure in Fig. 3(d) demonstrates two such hourglass nodal points as indicated by dashed circles, which are very near to the Fermi level. Based on low-energy model analysis [51], these hourglass nodal points are found to be Weyl points. Then we present Sr_2Bi_3 [58] as an hourglass material example, which crystallizes in SG 52 owning an inversion center with a primitive orthorhombic lattice. The BZ is shown in Fig. 3(b) and the electronic band structure by first-principles

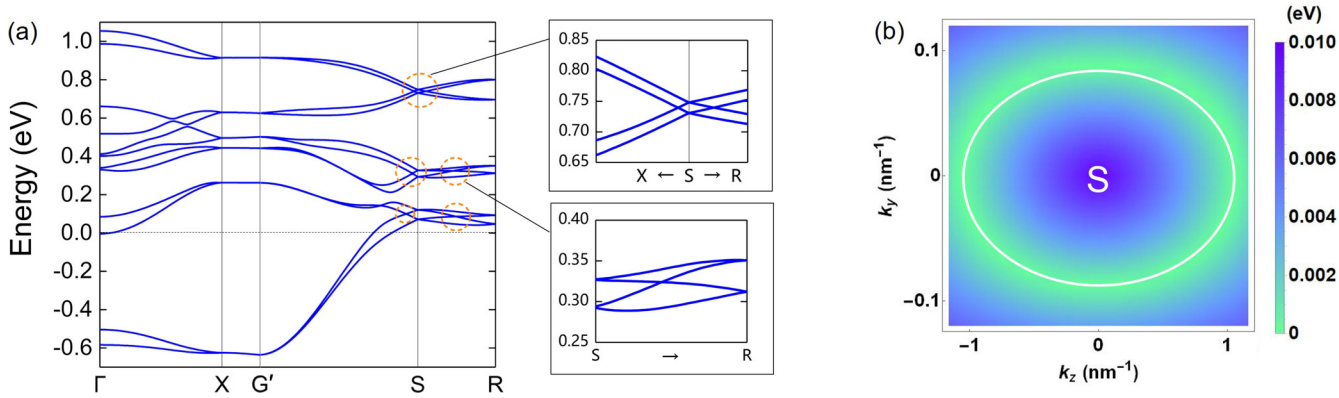

FIG. 4. (a) The electronic band structure of Ba_2ReO_5 where G′ is the middle point of UX. Note that the bands in X-G′ are always fourfold degenerate since only one four-dimensional irrep is allowed in HSL G. In fact, any path (even not a straight line) connecting S and any point in HSL G could host essential hourglass BC. We highlight six hourglass BCs in the band structure with two of them enlarged, shown in the right-side insets. (b) The expected hourglass nodal loop (the white loop) around S in the L plane is verified by our first-principles calculations.

calculations is shown in Fig. 3(e). Because SG 52 owns an inversion center, each band should be doublefold degenerate. The fourfold degenerate essential hourglass nodal point in D is indicated by an orange dashed circle and is found to be a Dirac point [51].

Other than achrial hourglass materials as above, for SG 182 we present ReO_3 [59] which could host a chiral and essential hourglass nodal point. Such an hourglass nodal point must appear in HSL U, connecting L and M, shown in the BZ of Fig. 3(c). The electronic band structure of ReO_3 by first-principles calculations is displayed in Fig. 3(f), where we highlight three such hourglass Weyl points by dashed circles. Note that for the highest dashed circle, there exists an additional BC (denoted by an red arrow) other than the hourglass one (denoted by the black arrow) in the hourglass structure in the band plot. Such a BC is not robust to external strain, unlike the hourglass BC, and can be tuned to be gapped easily as schematically shown in the inset of Fig. 3(f).

B. Material with essential hourglass nodal line

We have listed all positions of essential hourglass nodal lines in Table IV. As shown in Table IV, for SG 62 with primitive orthorhombic lattice there is an hourglass nodal line in L($k_x = \frac{\pi}{a}$) plane [i.e., UXSR plane in Fig. 3(b)]. As an example, we show that Ba_2ReO_5 in SG 62 could host such an hourglass nodal line. We find that S-D-X and S-Q-R could host essential hourglass BCs where D and Q are both HSLs. However, we find that the hourglass BC in D or Q actually lies in a nodal line in the L plane. Actually, S-L-G, S-L-P, S-L-R,S-L-U,S-L-X are all found to display essential hourglass nodal lines by our criteria described in Secs. II and III. Above all, we expect a nodal loop around S in plane L to emerge. The first-principles calculated band structure of Ba_2ReO_5 [60] is shown in Fig. 4(a) where six hourglass BCs near the Fermi level are shown. Any energy band is doublefold degenerate for SG 62 is centrosymmetric. Besides, the bands in HSL G (G′X) are always fourfold degenerate [50] as shown in the first-principles calculated band structure in Fig. 4(a). The path connecting S and any point in G could host an hourglass BC, which finally could constitute a Dirac nodal line. As displayed in Fig. 4(b), such a Dirac nodal loop obtained through first-principles calculations is around S in the L plane. Furthermore, it is found that the Dirac nodal loop owns a very narrow band width, being only about 13.6 meV based on our first-principles results. It is also worth mentioning that any path in L which connects S and an arbitrary point in P can host an hourglass BC, which is shown in the SM [51].

V. CONCLUSIONS AND PERSPECTIVES

Based on the compatibility relations from the Bilbao server [50], we obtain all the possible hourglass BCs in the BZ of all 230 SGs. We consider not only double valued representations but also single-valued representations. They are suitable for electronic materials with significant SOC, and negligible SOC, or bosonic systems (e.g., phonon, photon or magnon systems), respectively. Furthermore, we also consider situations with/without TRS for nonmagnetic/magnetic materials. We highlight hourglass BCs which are essential, for they are very promising to be used to realize materials with hourglass BCs near the Fermi level. The SGs where the essential hourglass structure exists are all nonsymmorphic groups. Based on the essential results, we predict several hourglass materials which are expected to be synthesized for further studies.

It is worth pointing out that several other special occasions (for example, R and B are related by symmetry, or even differently by a reciprocal lattice vector) which can also host hourglass BCs are not captured in our search since their compatibility relations are not explicitly listed on the Bilbao server [50]. However, our methodology can be directly applied to these cases. Although we apply our results to show an hourglass band structure in nonmagnetic materials, they can also be applied to magnetic materials or even bosonic systems. In addition, since the layer group or rod group is a subgroup of SG, our results can also be used to search hourglass materials in lower dimensions. Finally, our method can be applied to type-III or -IV magnetic SGs, for which the missing essential type-b hourglass BCs in our work, which is only based on 230 SGs, may be found.

ACKNOWLEDGMENTS

We were supported by the National Key R&D Program of China (Grants No. 2017YFA0303203 and No. 2018YFA0305704), the National Natural Science Foundation of China (NSFC Grants No. 11525417, No. 11834006, No. 51721001, and No. 11790311) and the excellent program at Nanjing University. X.W. also acknowledges the support from the Tencent Foundation through the XPLORER PRIZE. F.T. was supported by the Fundamental Research Fund for the Central Universities (No. 14380144) and thanks Prof. Dingyu Xing and Prof. Baigen Wang for their kind and substantial support on scientific research.

[1] X.-L. Qi and S.-C. Zhang, Topological insulators and superconductors, Rev. Mod. Phys. **83**, 1057 (2011).

[2] M. Z. Hasan and C. L. Kane, *Colloquium:* Topological insulators, Rev. Mod. Phys. **82**, 3045 (2010).

[3] A. Bansil, H. Lin, and T. Das, *Colloquium:* Topological band theory, Rev. Mod. Phys. **88**, 021004 (2016).

[4] Y. Ando and L. Fu, Topological crystalline insulators and topological superconductors: From concepts to materials, Annu. Rev. Condens. Matter Phys. **6**, 361 (2015).

[5] N. P. Armitage, E. J. Mele, and A. Vishwanath, Weyl and Dirac semimetals in three-dimensional solids, Rev. Mod. Phys. **90**, 015001 (2018).

[6] A. P. Schnyder, S. Ryu, A. Furusaki, and A. W. W. Ludwig, Classification of topological insulators and superconductors in three spatial dimensions, Phys. Rev. B **78**, 195125 (2008).

[7] A. Kitaev, Periodic table for topological insulators and superconductors, in *Advances in Theoretical Physics: Landau Memorial Conference*, edited by V. Lebedev and M. Feigel'man, AIP Conf. Proc. No. 1134 (AIP, New York, 2008), p. 22.

[8] S. Ryu, A. P. Schnyder, A. Furusaki, and A. W. W. Ludwig, Topological insulators and superconductors: Tenfold way and dimensional hierarchy, New J. Phys. **12**, 065010 (2010).

[9] J. Kruthoff, J. de Boer, J. van Wezel, C. L. Kane, and R.-J. Slager, Topological classification of crystalline insulators through band structure combinatorics, Phys. Rev. X **7**, 041069 (2017).

[10] X. Wan, A. M. Turner, A. Vishwanath, and S. Y. Savrasov, Topological semimetal and fermi-arc surface states in the electronic structure of pyrochlore iridates, Phys. Rev. B **83**, 205101 (2011).

[11] G. Xu, H. Weng, Z. Wang, X. Dai, and Z. Fang, Chern Semimetal and the Quantized Anomalous Hall Effect in $HgCr_2Se_4$, Phys. Rev. Lett. **107**, 186806 (2011).

[12] H. Weng, C. Fang, Z. Fang, B. A. Bernevig, and X. Dai, Weyl Semimetal Phase in Noncentrosymmetric Transition-Metal Monophosphides, Phys. Rev. X **5**, 011029 (2015).

[13] S.-M. Huang, S.-Y. Xu, I. Belopolski, C.-C. Lee, G. Chang, B. Wang, N. Alidoust, G. Bian, M. Neupane, and C. Z *et al.*, A Weyl fermion semimetal with surface fermi arcs in the transition metal monopnictide TaAs class, Nat. Commun. **6**, 7373 (2015).

[14] S. M. Young, S. Zaheer, J. C. Y. Teo, C. L. Kane, E. J. Mele, and A. M. Rappe, Dirac Semimetal in Three Dimensions, Phys. Rev. Lett. **108**, 140405 (2012).

[15] Z. Wang, Y. Sun, X.-Q. Chen, C. Franchini, G. Xu, H. Weng, X. Dai, and Z. Fang, Dirac semimetal and topological phase transitions in A_3 Bi (A=Na, K, Rb), Phys. Rev. B **85**, 195320 (2012).

[16] Z. Wang, H. Weng, Q. Wu, X. Dai, and Z. Fang, Three-dimensional Dirac semimetal and quantum transport in Cd_3As_2, Phys. Rev. B **88**, 125427 (2013).

[17] Y. Du, B. Wan, D. Wang, L. Sheng, C.-G. Duan, and X. Wan, Dirac and Weyl semimetal in XYBi (X = Ba, Eu; Y = Cu, Ag and Au), Sci. Rep. **5**, 14423 (2015).

[18] B. Bradlyn, J. Cano, Z. Wang, M. G. Vergniory, C. Felser, R. J. Cava, and B. A. Bernevig, Beyond Dirac and Weyl fermions: Unconventional quasiparticles in conventional crystals, Science **353**, aaf5037 (2016).

[19] P. Tang, Q. Zhou, and S.-C. Zhang, Multiple types of Topological Fermions in Transition Metal Silicides, Phys. Rev. Lett. **119**, 206402 (2017).

[20] G. Chang, S.-Y. Xu, B. J. Wieder, D. S. Sanchez, S.-M. Huang, I. Belopolski, T.-R. Chang, S. Zhang, A. Bansil, and H. L. *et al.*, Unconventional Chiral Fermions and Large Topological Fermi Arcs in RhSi, Phys. Rev. Lett. **119**, 206401 (2017).

[21] H. Weng, C. Fang, Z. Fang, and X. Dai, Topological semimetals with triply degenerate nodal points in θ-phase tantalum nitride, Phys. Rev. B **93**, 241202(R) (2016).

[22] B. Q. Lv, Z.-L. Feng, Q.-N. Xu, X. Gao, J.-Z. Ma, L.-Y. Kong, P. Richard, Y.-B. Huang, V. N. Strocov, and C. F *et al.*, Observation of three-component fermions in the topological semimetal molybdenum phosphide, Nature **546**, 627 (2017).

[23] A. A. Burkov, M. D. Hook, and L. Balents, Topological nodal semimetals, Phys. Rev. B **84**, 235126 (2011).

[24] R. Yu, H. Weng, Z. Fang, X. Dai, and X. Hu, Topological Node-Line Semimetal and Dirac Semimetal State in Antiperovskite Cu_3 PdN, Phys. Rev. Lett. **115**, 036807 (2015).

[25] Y. Kim, B. J. Wieder, C. L. Kane, and A. M. Rappe, Dirac Line Nodes in Inversion-Symmetric Crystals., Phys. Rev. Lett. **115**, 036806 (2015).

[26] C. Fang, Y. Chen, H.-Y. Kee, and L. Fu, Topological nodal line semimetals with and without spin-orbital coupling, Phys. Rev. B **92**, 081201(R) (2015).

[27] Y. Du, F. Tang, D. Wang, L. Sheng, E.-J. Kan, C.-G. Duan, S. Y. Savrasov, and X. Wan, CaTe: A new topological node-line and Dirac semimetal, npj Quantum Mater. **2**, 3 (2017).

[28] T. Bzdušek, Q. S. Wu, A. Ruegg, M. Sigrist, and A. A. Soluyanov, Nodal-chain metals, Nature **538**, 75 (2016).

[29] W. Chen, H.-Z. Lu, and J.-M. Hou, Topological semimetals with a double-helix nodal link, Phys. Rev. B **96**, 041102(R) (2017).

[30] Z. Yan, R. Bi, H. Shen, L. Lu, S.-C. Zhang, and Z. Wang, Nodal-link semimetals, Phys. Rev. B **96**, 041103(R) (2017).

[31] M. Ezawa, Topological semimetals carrying arbitrary Hopf numbers: Fermi surface topologies of a Hopf link, Solomon's knot, Trefoil knot, and other linked nodal varieties, Phys. Rev. B **96**, 041202(R) (2017).

[32] P.-Y. Chang and C.-H. Yee, Weyl-link semimetals, Phys. Rev. B **96**, 081114(R) (2017).

[33] Z. Wang, A. Alexandradinata, R. J. Cava, and B. A. Bernevig, Hourglass fermions, Nature **532**, 189 (2016).

[34] L. Wang, S.-K. Jian, and H. Yao, Hourglass semimetals with nonsymmorphic symmetries in three dimensions, Phys. Rev. B **96**, 075110 (2017).
[35] S.-S. Wang, Y. Liu, Z.-M. Yu, X.-L. Sheng, and S. A. Yang, Hourglass Dirac chain metal in rhenium dioxide, Nat. Commun. **8**, 1844 (2017).
[36] Y. Chen, H.-S. Kim, and H.-Y. Kee, Topological crystalline semimetals in nonsymmorphic lattices, Phys. Rev. B **93**, 155140 (2016).
[37] M. Ezawa, Hourglass fermion surface states in stacked topological insulators with nonsymmorphic symmetry, Phys. Rev. B **94**, 155148 (2016).
[38] R. Takahashi, M. Hirayama, and S. Murakami, Spinless hourglass nodal-line semimetals, Phys. Rev. B **96**, 155206 (2017).
[39] J. Zhang, Y.-H. Chan, C.-K. Chiu, M. G. Vergniory, L. M. Schoop, and A. P. Schnyder, Topological band crossings in hexagonal materials, Phys. Rev. Mater. **2**, 074201 (2018).
[40] Y.-H. Chan, B. Kilic, M. M. Hirschmann, C.-K. Chiu, L. M. Schoop, D. G. Joshi, and A. P. Schnyder, Symmetry-enforced band crossings in trigonal materials: Accordion states and Weyl nodal lines, Phys. Rev. Mater. **3**, 124204 (2019).
[41] W. Wu, Y. Jiao, S. Li, X.-L. Sheng, Z.-M. Yu, and S. A. Yang, Hourglass Weyl loops in two dimensions: Theory and material realization in monolayer GaTeI family, Phys. Rev. Mater. **3**, 054203 (2019).
[42] B. J. Wieder and C. L. Kane, Spin-orbit semimetals in layer groups, Phys. Rev. B **94**, 155108 (2016).
[43] C. Chen, Z.-M. Yu, S. Li, Z. Chen, X.-L. Sheng, and S. A. Yang, Weyl-loop half-metal in $Li_3(FeO_3)_2$, Phys. Rev. B **99**, 075131 (2019).
[44] B. Fu, X. Fan, D. Ma, C.-C. Liu, and Y. Yao, Hourglasslike nodal net semimetal in Ag_2 BiO_3, Phys. Rev. B **98**, 075146 (2018).
[45] B. Singh, B. Ghosh, C. Su, H. Lin, A. Agarwal, and A. Bansil, Topological Hourglass Dirac Semimetal in the Nonpolar Phase of Ag_2 BiO_3, Phys. Rev. Lett. **121**, 226401 (2018).
[46] S. Li, Y. Liu, S.-S. Wang, Z.-M. Yu, S. Guan, X.-L. Sheng, Y. Yao, and S. A. Yang, Nonsymmorphic-symmetry-protected hourglass Dirac loop, nodal line, and Dirac point in bulk and monolayer X_3 $SiTe_6$(X=Ta, Nb), Phys. Rev. B **97**, 045131 (2018).
[47] D. Shao, H. Wang, T. Chen, P. Lu, Q. Gu, L. Sheng, D. Xing, and J. Sun, Composite topological nodal lines penetrating the Brillouin zone in orthorhombic AgF_2, npj Comput. Mater. **5**, 53 (2019).
[48] F. Tang, H. C. Po, A. Vishwanath, and X. Wan, Efficient topological materials discovery using symmetry indicators, Nat. Phys. **15**, 470 (2019).
[49] Y.-T. Oh, H.-G. Min, and Y. Kim, Dual topological nodal line and nonsymmorphic Dirac semimetal in three dimensions, Phys. Rev. B **99**, 201110(R) (2019).
[50] http://www.cryst.ehu.es.
[51] See Supplemental Material at http://link.aps.org/supplemental/10.1103/PhysRevB.102.035106 which contains the analyses of the essential hourglass nodal points and nodal loop for crystals shown in the main text by conventional operator algebra method, and an exhaustive list of all possible hourglass BCs for systems with/without TRS and with significant/negligible SOC. The exhaustive list shows the position, splitting pattern and type of each hourglass band structure, and the essential BCs are highlighted in red.
[52] Y. Li and Y. Ma, Crystal structure and physical properties of OsN: First-principle calculations, Solid State Commun. **150**, 759 (2010).
[53] P. Chai and J. D. Corbett, Two new compounds, β-ScTe and Y_3Au_2, and a reassessment of Y_2Au, Acta Cryst. C **67**, i53 (2011).
[54] P. Blaha, K. Schwarz, G. K. H. Madsen, D. Kvasnicka, J. Luitz, R. Laskowski, F. Tran, and L. Marks, *Wien2k, an Augmented Plane Wave + Local Orbitals Program for Calculating Crystal Properties* (Karlheinz Schwarz, Technische Univ. Wien, Austria, 2001).
[55] J. P. Perdew, K. Burke, and M. Ernzerhof, Generalized Gradient Approximation Made Simple, Phys. Rev. Lett. **77**, 3865 (1996).
[56] G. Chang, B. J. Wieder, F. Schindler, D. S. Sanchez, I. Belopolski, S.-M. Huang, B. Singh, D. Wu, T.-R. Chang, and Titus Neupert *et al.*, Topological quantum properties of chiral crystals, Nat. Mater. **17**, 978 (2018).
[57] P. Matkovic and T. Matkovic, A new intermetallic phase in the Pd-Pb-As system, J. Alloys Compounds **202**, 107 (1993).
[58] F. Merlo and M. L. Fornasini, Crystal structure of some phases and alloying behavior in alkaline earths, europium and ytterbium pnictides, Mater. Res. Bull. **29**, 149 (1994).
[59] T. I. Dyuzheva, N. A. Bendeliani, and S. S. Kabalkina, New high-pressure phases of ReO_3, J. Less Common Met. **133**, 313 (1987).
[60] A. K. Cheetham and D. M. Thomas, An investigation of the low oxidation state chemistry of rhenium in the BaO-Re-Re_2O_7 phase diagram, J. Solid State Chem. **71**, 61 (1987).